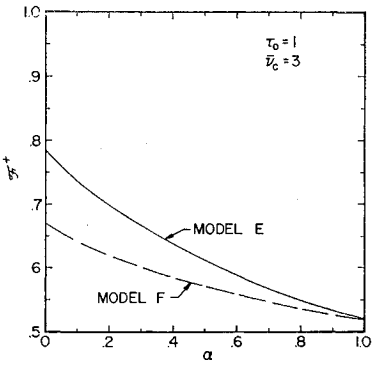

Fig. 2 Effect of α on the radiative flux for models E and F, $\theta_1 = 0.5$, $\bar{\nu}_c = 3$, $\tau_o = 1$.

greater than the gray case for $\alpha \geq 0.26$. The maximum value of the temperature [$\theta(0) \simeq 0.741$] occurs near $\alpha = 0.5$. The situation is reversed at $\tau = 1$. The temperature for model F has a minimum near $\alpha = 0.5$, and $\theta(\tau_o)$ for model E is almost linear with α. For any given value of $\alpha < 1$ and any τ, the temperature for model F is always greater than that for model E.

The numerical values for $\mathfrak{F}^+$ are given in Tables 2 and 3 as well as illustrated graphically in Fig. 2. For all values of $\alpha \geq 0$, the energy transferred between the plates is greatest for model E. As expected, for both models the radiative flux is a monotonically decreasing function of α and reduces to the gray result for $\alpha = 1$.

References

[1] Crosbie, A. L. and Viskanta, R., "The Exact Solution to a Simple Nongray Radiative Transfer Problem," *Journal of Quantitative Spectroscopy and Radiative Transfer*, Vol. 9, 1969, pp. 553–568.

[2] Crosbie, A. L., "Radiation Heat Transfer in a Nongray Planar Medium," Ph.D. thesis, 1969, Purdue University.

An Extension to Existing Methods of Determining Refractive Indices from Axisymmetric Interferograms

ROBERT SOUTH*
The Gas Council, Watson House, London, England

Nomenclature

N = refractive index in disturbance
N_o = refractive index in reference field
r = radius $= (x^2 + y^2)^{1/2}$
R_0 = radius of axisymmetric disturbance
S = fringe shift
x,y,z = rectangular coordinates, with x in the direction of the light beam and z the axis of symmetry
λ = vacuum wavelength of light

1. Introduction

IT is often required to determine the density or temperature in an axisymmetric system, such as the flow field around a missile, or the mass transfer field in a jet. For obvious reasons optical methods are particularly suitable for making measurements of this sort and interferometry, in particular, has found wide application.

Received May 12, 1970; revision received June 29, 1970. The author would like to thank J. P. Price for advice and assistance on the foregoing mathematics and also the Gas Council and the City University for permission to publish this paper.

* Research Physicist, Combustion Research Group.

Various methods have been evolved for analyzing axisymmetric interferograms, and these are generally satisfactory when the fringe shift distribution is a simple function of lateral distance. However, when the fringe shift distribution is relatively complex, as is the case for interferograms of axisymmetric laminar diffusion flames, the existing methods are not entirely satisfactory. The foregoing problem has led the author to develop a method of analyzing interferograms of axisymmetric laminar flames, and the method developed would appear to be altogether more generally applicable than existing methods.

2. Existing Methods

A fringe shift results from the difference in optical path of two light beams, one of which passes through the refractive index disturbance and the other through a reference refractive index field. If the disturbance shows axial symmetry about, say, the z axis, the fringe shift, which is the difference in wavelengths of the optical paths of the two light beams, is given by

$$S(y) = \frac{1}{\lambda}\int_{x_1}^{x_2} [N(x) - N_0]dx \tag{1}$$

where x is in the direction of the light beam. In polar coordinates Eq. (1) becomes

$$S(y) = \frac{2}{\lambda}\int_{y}^{R_0} [N(r) - N_0]rdr/(r^2 - y^2)^{1/2} \tag{2}$$

where, Fig. 1, $r = (x^2 + y^2)^{1/2}$, and R_0 is the radius of the disturbance, i.e., where $N(r) = N_0$.

If the functions are suitably well behaved, then by Abel's transformation Eq. (2) becomes

$$N(r) - N_0 = -\frac{\lambda}{\pi r}\frac{d}{dr}\int_{r}^{R_0} \frac{S(y)ydy}{(y^2 - r^2)^{1/2}} \tag{3}$$

Freeman and Katz[1] have used Eq. (3) for analyzing radiance profiles in plasma discharges for those cases where the data can be fitted by least squares to a simple functional form.

Bradley[2] used a similar approach in which the observed fringe shift distribution is represented in the unit interval by a cubic and the coefficients are determined by a least squares fit of the observed fringe shift values.

However, the solutions discussed above and the forerunners of these[3–5] are not particularly suitable for those cases, such as the analysis of axisymmetric flames, where the observed fringe shift distribution is a relatively complex function of lateral distance.

3. A More General Approach

We now propose an extension to the existing approaches that is suitable for cases where the complete observed lateral fringe shift distribution cannot adequately be represented within experimental error of the data by a single curve of sufficiently low order. To be acceptable, a representation should be reasonably low-ordered, correlate the data to within experimental error, and introduce no unwarranted inflection points.

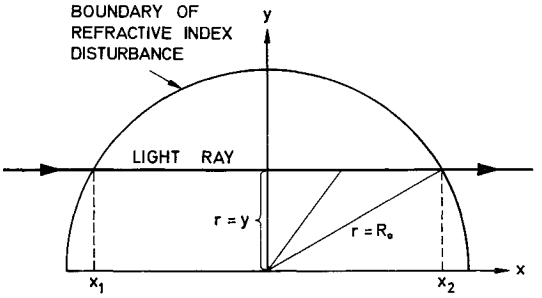

Fig. 1 Axisymmetric refractive index disturbance traversed by a light beam.

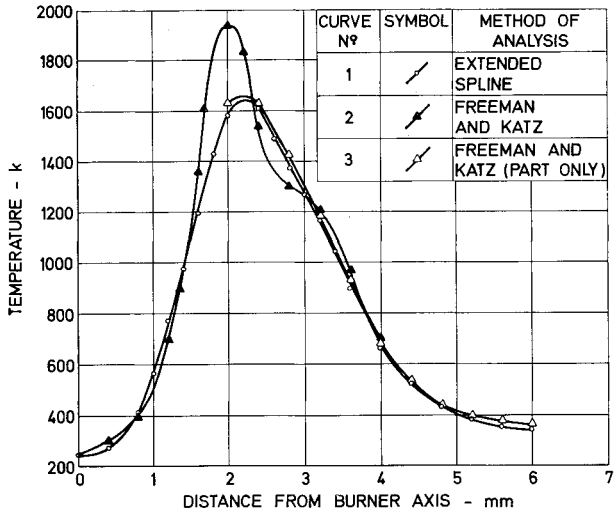

a) Comparison between the extended spline approach adopted by author (curve 1), and the Freeman and Katz approach (curves 2 and 3)

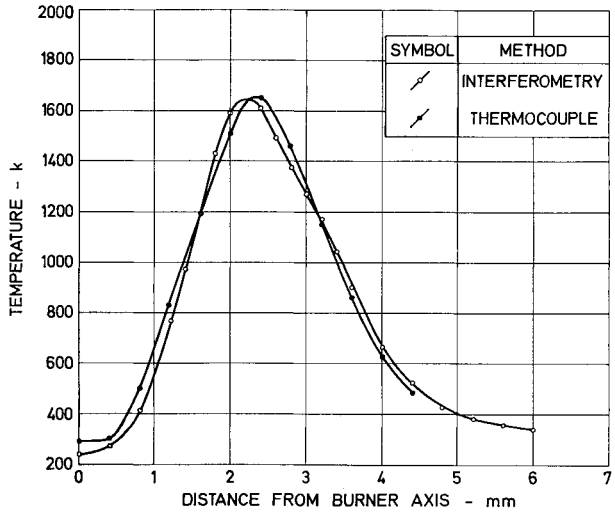

b) Comparison between the extended spline approach adopted by Author and a thermocouple probe method

Fig. 2 Radial temperature distributions.

Let the observed lateral fringe shift distribution be represented by low-order polynomials, in sections, using an extension of the Spline Fit Technique.[6] The sectional boundaries or knots are necessarily determined arbitrarily such that each interval may contain a number of data points. Generally, a cubic is used to represent the data within each section, constraints being placed on the cubics such that at each knot the adjacent cubics give the same values for the dependent variable and its first two derivatives. The usual constraint that the sum of the squares of the deviations between experimental and analytical data be a minimum is also made to apply.

Consider a section $p, p+1$ such that $R_{p+1} < r < R_p$ and let

$$S(y) = \sum_{i=0}^{3} C_i(R_p^2 - y^2)^i \tag{4}$$

Equation (3) then becomes

$$N(r) - N_0 = -\frac{\lambda}{\pi r}\frac{d}{dr}\left[\int_r^{R_p} \frac{S(y)_{p,p+1}ydy}{(y^2 - r^2)^{1/2}} + \sum_{n=1}^{p}\int_{R_n}^{R_{n-1}} \frac{S(y)_{n-1,n}ydy}{(y^2 - r^2)^{1/2}}\right] \tag{5}$$

where $S(y)_{p,p+1}$ is the analytical representation of data within section $p, p+1$. Equation (5) then becomes by straightforward integration or otherwise

$$N(r) - N_0 = \lambda\left\{\left[\sum_{i=0}^{3} A_iC_i(R_p^2 - r^2)^{i-1/2}\right] + \sum_{n=1}^{p}\sum_{i=0}^{3} C_i\left(A_i[(R_{n-1}^2 - r^2)^{i-1/2} - (R_n^2 - r^2)^{i-1/2}] - \sum_{j=1}^{i}\frac{(R_{n-1}^2 - R_n^2)^{i-j+1}(R_n^2 - r^2)^{j-3/2}\,2^{2(j-1)}i!(j-1)!}{\pi(i-j+1)!\;(2j-2)!}\right)\right\} \tag{6}$$

where $A_i = (2^{2i}/\pi)[(i!)^2/(2i)!]$

4. Assessment of the New Approach

The merit of the foregoing approach is that the method of analysis lends itself to cases where the complete observed lateral fringe shift distributions cannot adequately be represented by a polynomial of sufficiently low order.

A comparison with the existing method of Freeman and Katz is illustrated in Fig. 2a. A lateral fringe shift distribution was analyzed in three separate ways for refractive index. The resultant refractive indices were then related to flame temperature, a correction being made for the secondary dependence of refractive index on composition changes in the flame.[5]

Curve 1, Fig. 2a, was computed using the extended approach. Curve 2 was computed using a complete representation of the observed fringe shifts by the method of Freeman and Katz. Curve 3 was computed by restricting the method of Freeman and Katz to the outermost part of the flame. A comparison between curves 1 and 3 shows that the extended method and the existing method of Freeman and Katz show good agreement over the outermost part of the flame. However, curve 2 shows a breakdown in the adequacy of a single curve representation of the observed fringe shift data. Curve 1 shows a shape close to that to be expected.

But how close this is to the actual temperature distribution is not easy to establish because alternative methods that might be used to measure the temperature distribution are probably no more reliable than the method used to obtain Curve 1. However, some measure of cross checking was provided by thermocouple measurements using a couple constructed by butt-welding 0.0025 cm diam wires of Pt/20% Rh and Pt/40% Rh and coating with silica. As may be seen in Fig. 2b, the agreement between the temperature distributions obtained by thermocouple and by the extended spline analysis of an interferogram is satisfactory.

5. Conclusions

It has been shown that an Extended Spline Fit Technique can be adapted for the analysis of axisymmetric interferograms of laminar diffusion flames. Indeed, the proposed method could be applied to many other situations where the observed fringe shift distributions of axisymmetric interferograms are a relatively complex function of lateral distance.

References

[1] Freeman, M. P. and Katz, S., "Determination of a Radiance-Coefficient Profile from the Observed Asymmetric Radiance Distribution of an Optically Thin Radiating Medium," *Journal of the Optical Society of America*, Vol. 53, No. 10, Oct. 1963, pp. 1172–1179.

[2] Bradley, J. W., "Density Determination from Axisymmetric Interferograms," *AIAA Journal*, Vol. 6, No. 6, June 1968, pp. 1190–1192.

[3] Bennet, F. D., Carter, W. C., and Bergdolt, V. E., "Interferometric Analysis of Airflow about Projectiles in Free Flight," *Journal of Applied Physics*, Vol. 23, No. 4, April 1952, pp. 453–469.

[4] Ladenburg, R., Van Voorhis, C. C., and Winckler, J., "Interferometric Studies of Faster than Sound Phenomena. Part II.

Analysis of Supersonic Air Jets," *Physical Review*, Vol. 76, No. 5, Sept. 1, 1949, pp. 662–677.

[5] Pandya, T. P. and Weinberg, F. J., "The Study of the Structure of Laminar Diffusion Flames by Optical Methods," 9th International Symposium on Combustion, 1963, pp. 587–596.

[6] Klaus, R. L. and Van Ness, H. C., "An Extension of the Spline Fit Technique and Applications to Thermodynamic Data," *AIChE Journal*, Vol. 13, No. 6, Nov. 1967, pp. 1132–1136.

Experimental Study of Wind-Wave Interaction

Y. S. Lou* and B. S. Seidel†
University of Delaware, Newark, Del.

Introduction

THIS brief Note is written to report some of the experimental results of the study on the generation of water surface waves by wind. Various theoretical and experimental investigations have been performed in the past.[1–11] Interest in the problem dates from the work of Helmholtz[1] and Kelvin[2] whose mathematical modelling of the flow yielded a prediction for the critical wind velocity, or as it is called, the onset of instability, required to generate surface waves. For air over water this prediction yields a value of 21.3 fps. On the open ocean or lake, observations show that the critical velocity is rather nearer 0.68 fps. In a recent paper,[3] in which the air is modelled as stratified, two critical velocities are revealed; one at 0.705 fps (the "initial instability") and the second at 19.9 fps (the "gross instability"). Laboratory observations have ranged from 0.722 fps to as high as 21.35 fps for different depths of water. This Note reviews these measurements as well as reports on an investigation of the influence of corrugated bottom geometry on the critical wind velocity.

Experimental Apparatus

A wind tunnel fitted with a water tank, shown in Fig. 1, was designed and built to study the critical velocities for instabilities at the wind-water interface. A "Flow Corporation" Model WT4 wind tunnel was used as an exhaust blower to produce air flow over the water. It is fitted with a base and supported by four helical springs to minimize vibration. The blower is equipped with a variable speed controller.

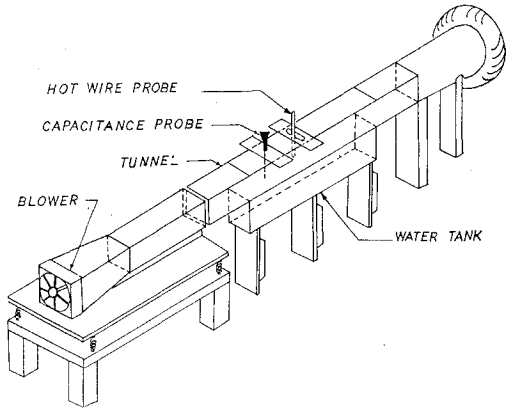

Fig. 1 Experimental apparatus.

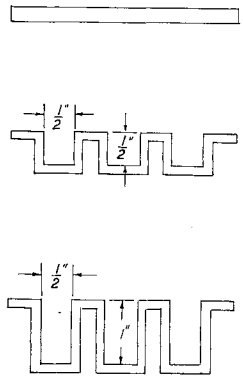

Fig. 2 Configurations of different shapes of beds.

The water tank section was fabricated from Plexiglas and it is 3.16 × 3.16 × 30 in. on top for air passage and fitted underneath with a 3.16 × 4 × 18 in. water tank. A variable bottom is supported by three screws so that the water depth may be varied. Tap water is introduced into the bottom of the water tank for fill and through a needle valve to the top of the water tank to compensate for evaporation.

Instrumentation and Experimental Procedures

The water tank is filled with tap water until the water level coincides with the inside bottom surface of the air passage. After the water level has settled, a capacitance probe is immersed 0.125 in. beneath the water surface. Flow of the airstream is then initiated in the tunnel and equilibrium conditions are allowed to be reached. The output signal of the capacitance probe due to change of the level of the water surface is sent into an oscilloscope and is recorded photographically. This procedure is performed over a range of air flow speeds for various water depths and three different shapes of beds (see Fig. 2). In every experiment these streamwise corrugations were totally immersed. For determining the velocity and the turbulent intensity level in the airstream corresponding to various settings of the flow controller, a constant temperature hot-wire anemometer system with a linearized anemometer unit is used. These measurements are made at various positions in the airstream above the water surface. In addition, the frequency spectrum of the air turbulence is obtained by recording the turbulent signal using a frequency modulated tape recorder, and then analyzing it with a wave analyzer. The turbulence spectrum is then recorded and reduced to energy per cycle as shown in Fig. 3. Because of the

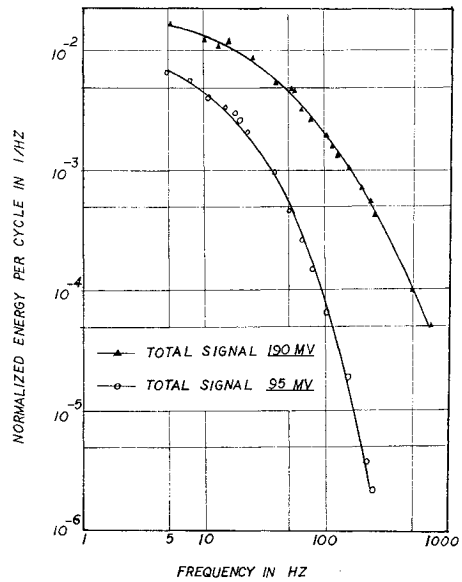

Fig. 3 Energy-frequency spectrum of turbulence in air stream.

Received April 28, 1970, revision received June 18, 1970.

* Associate Professor, Department of Mechanical and Aerospace Engineering. Member AIAA.

† Professor, Department of Mechanical and Aerospace Engineering. Associate Fellow AIAA.